

Cancer Cell, Volume 33

Supplemental Information

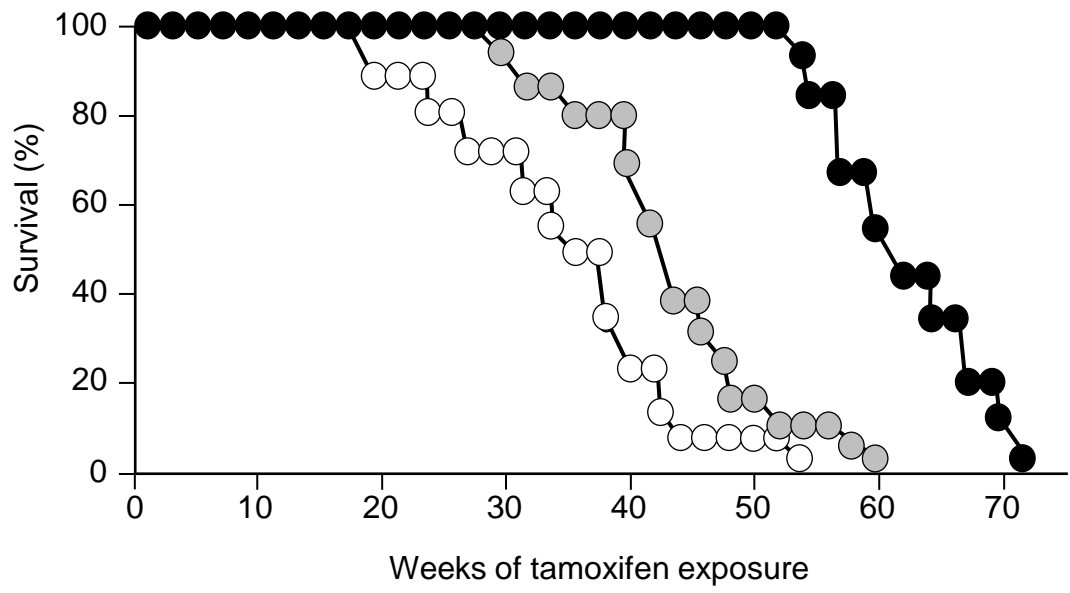
c-RAF Ablation Induces Regression of Advanced

***Kras/Trp53* Mutant Lung Adenocarcinomas**

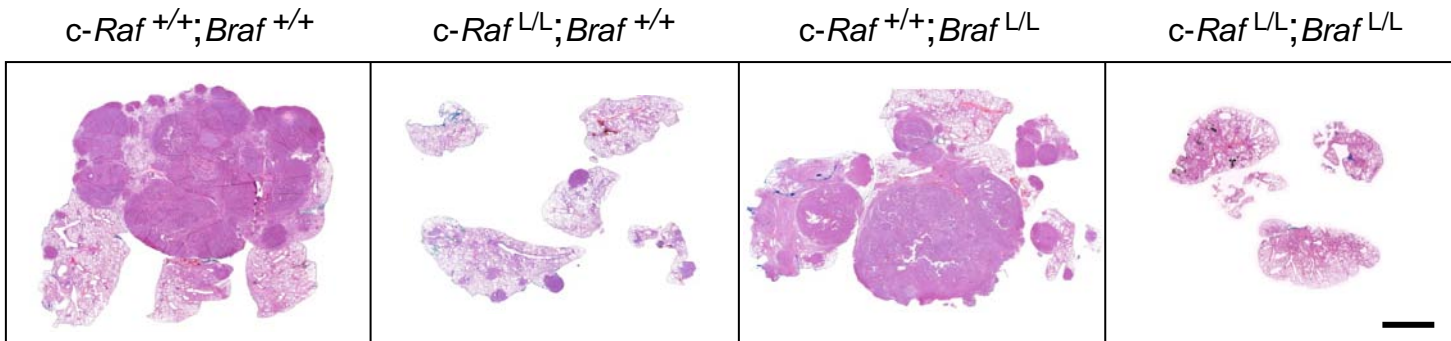
by a Mechanism Independent of MAPK Signaling

Manuel Sanclemente, Sarah Francoz, Laura Esteban-Burgos, Emilie Bousquet-Mur, Magdolna Djurec, Pedro P. Lopez-Casas, Manuel Hidalgo, Carmen Guerra, Matthias Drosten, Monica Musteanu, and Mariano Barbacid

A



B



C

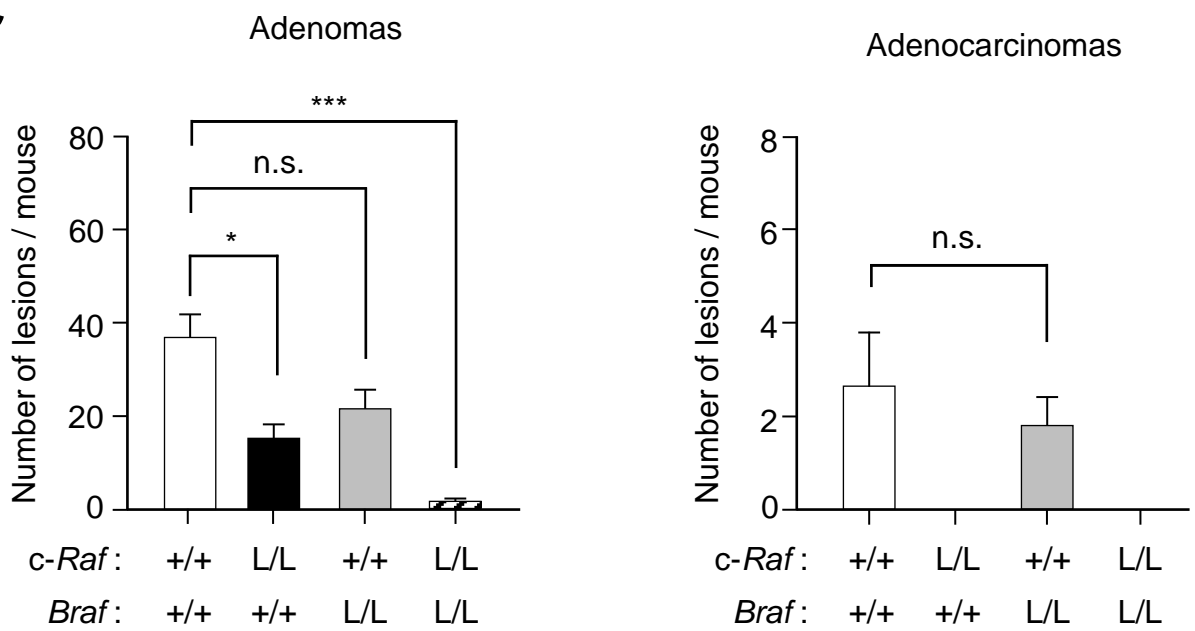


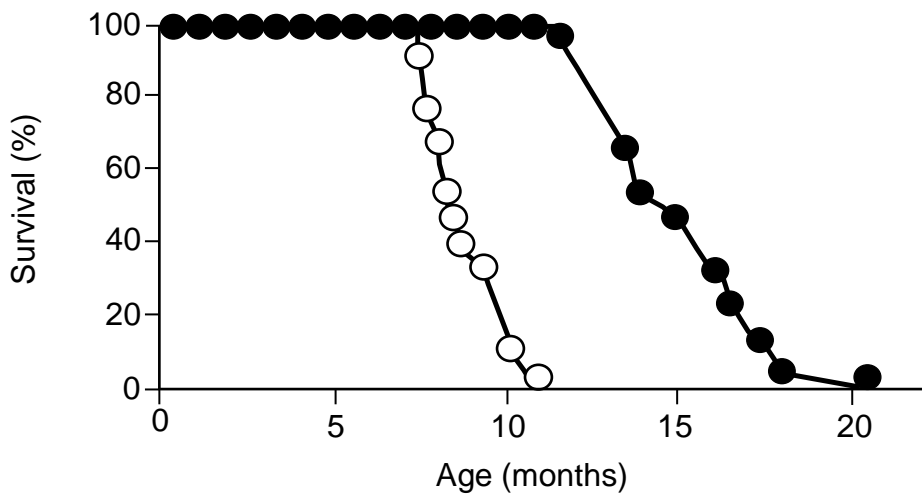
Figure S1. c-RAF ablation prevents progression of established *Kras*^{G12V} driven lung tumors. Related to Figure 3.

(A) Survival of *Kras*^{+ /FSFG12V}; *RERT*^{ert/ert} (n=18) (open circles), *Kras*^{+ /FSFG12V}; *RERT*^{ert/ert}; *Braf*^{L/L} (n=29) (solid grey circles), *Kras*^{+ /FSFG12V}; *RERT*^{ert/ert}; *c-Raf*^{L/L} (n=20) (solid black circles) CT⁺ tumor-bearing mice exposed to TMX for the indicated time. Mice were sacrificed at humane end point.

(B) H&E staining of paraffin sections of whole lungs obtained from representative *Kras*^{+ /FSFG12V}; *RERT*^{ert/ert}; *c-Raf*^{+/+}; *Braf*^{+/+}, *Kras*^{+ /FSFG12V}; *RERT*^{ert/ert}; *c-Raf*^{L/L}; *Braf*^{+/+}, *Kras*^{+ /FSFG12V}; *RERT*^{ert/ert}; *c-Raf*^{+/+}; *Braf*^{L/L} and *Kras*^{+ /FSFG12V}; *RERT*^{ert/ert}; *c-Raf*^{L/L}; *Braf*^{L/L} tumor bearing mice after 4 months of TMX exposure and sacrificed at humane end point. Scale bar, 5 mm.

(C) (Left) Quantification of number of adenomas and (Right) adenocarcinomas per mouse in *Kras*^{+ /FSFG12V}; *RERT*^{ert/ert}; *c-Raf*^{+/+}; *Braf*^{+/+} (open bar), *Kras*^{+ /FSFG12V}; *RERT*^{ert/ert}; *c-Raf*^{L/L}; *Braf*^{+/+} (solid black bar), *Kras*^{+ /FSFG12V}; *RERT*^{ert/ert}; *c-Raf*^{+/+}; *Braf*^{L/L} (solid grey bar) and *Kras*^{+ /FSFG12V}; *RERT*^{ert/ert}; *c-Raf*^{L/L}; *Braf*^{L/L} (stripped bar) tumor-bearing mice (n=6 per genotype) after 4 months of TMX exposure. Error bars indicate mean ± SEM. p values were calculated using the unpaired Student's T test. *p < 0.05, **p < 0.01 and ***p < 0.001. n.s.: not significant

A



B

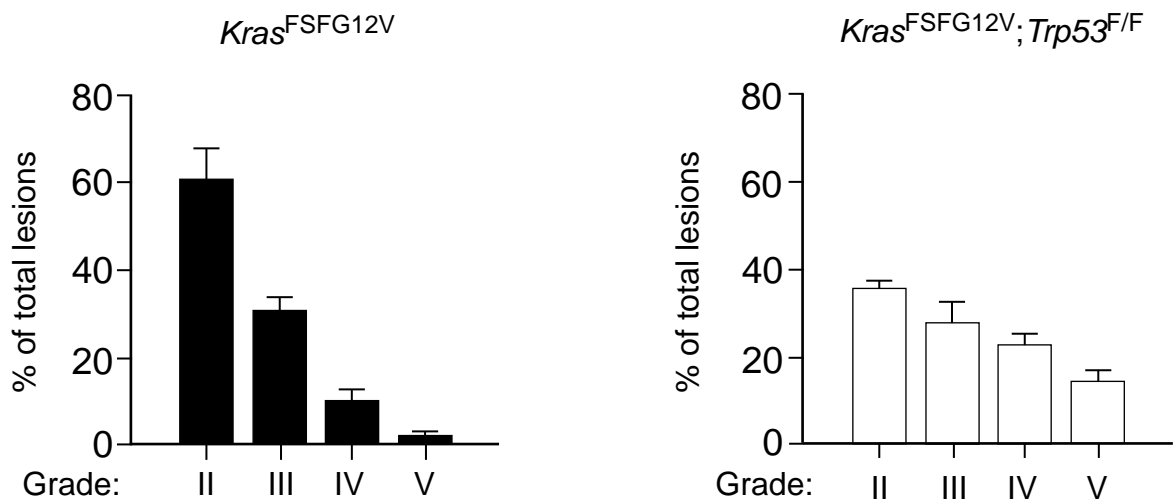


Figure S2. Survival and tumor grade in *Kras*^{+/FSFG12V} and *Kras*^{+/FSFG12V};*Trp53*^{F/F} mice upon infection with Ad-Flp particles. Related to Figure 3.

(A) Survival of *Kras*^{+/FSFG12V} (solid circles) (n=26) and *Kras*^{+/FSFG12V};*Trp53*^{F/F} (open circles) (n=21) infected with 10⁶ pfu of Ad-Flp/mouse at 2 months of age.

(B) Grading of tumors present in (Left) *Kras*^{+/FSFG12V} (solid bars) and (Right) *Kras*^{+/FSFG12V};*Trp53*^{F/F} (open bars) mice (n=6 per genotype) infected as indicated in (a) and sacrificed at humane end point. Results are indicated as percentage of grade II to V lesions. Error bars indicate mean ± SEM.

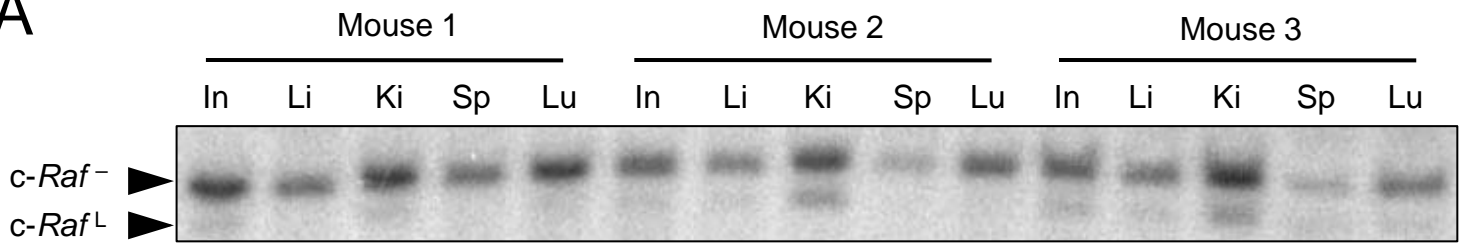
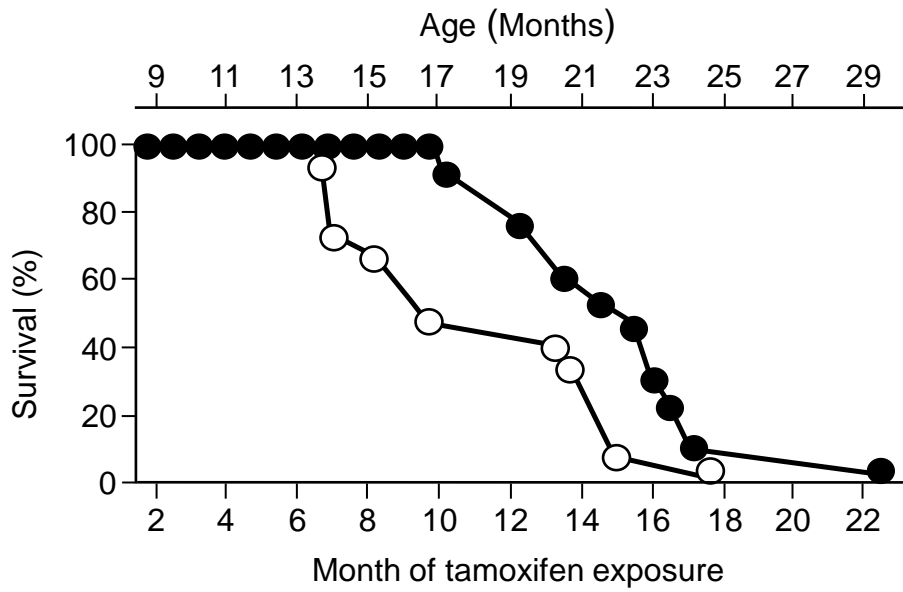
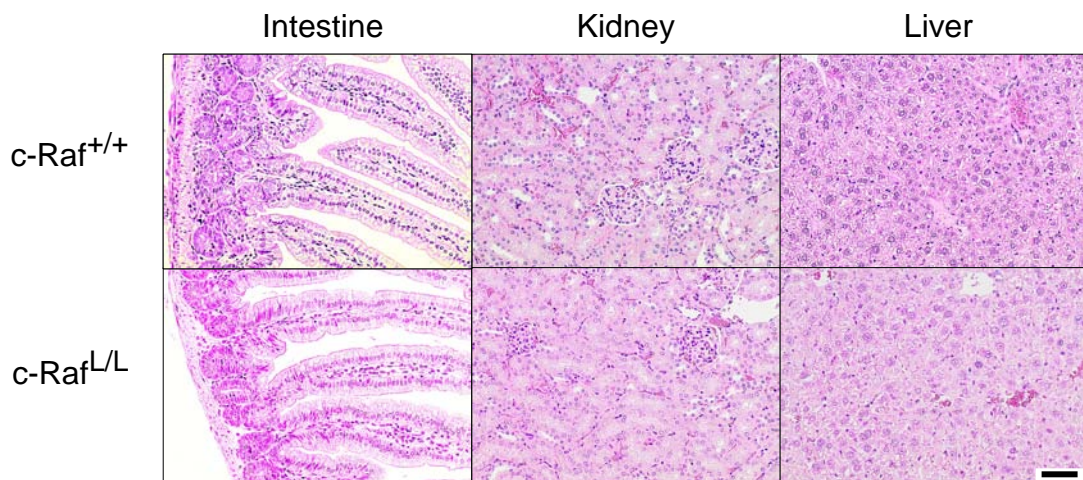
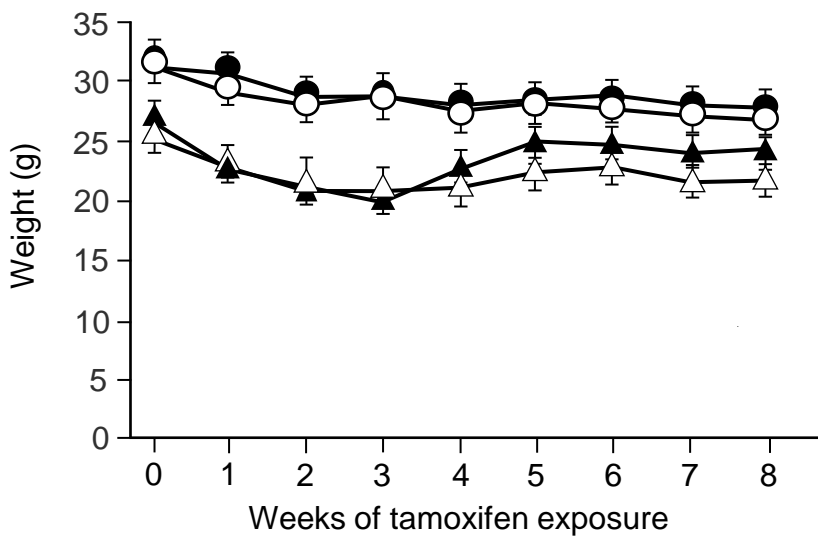
A**B****C****D****E**

Figure S3. c-RAF systemic ablation results in acceptable toxicity. Related to Figure 3.

(A) Southern blot analysis of $Kras^{+/FSFG12V};Trp53^{F/F};hUBC-CreERT2^{+/T};c-Raf^{L/L}$ tissues after 2 months of TMX exposure (n=3 mice). Migration of the diagnostic DNA fragments corresponding to the un-recombined $c-Raf^L$ (3.1 kbp) alleles as well as to the recombined $c-Raf^+$ (3.5 kbp) alleles are indicated by arrowheads. I: intestine, L: liver, K: kidney, S: spleen, Lu: lung.

(B) Survival of $Kras^{+/+};Trp53^{F/F};hUBC-CreERT2^{+/T};c-Raf^{+/+}$ (solid circles) (n=13) and $Kras^{+/+};Trp53^{F/F};hUBC-CreERT2^{+/T};c-Raf^{L/L}$ (open circles) (n=15) mice exposed to TMX *ad libitum*. Upper scale shows the animal age in months. Downer scale shows the time in months of TMX exposure.

(C) Representative photos of H&E stained histological sections of paraffin embedded organs of $Kras^{+/+};Trp53^{F/F};hUBC-CreERT2^{+/T};c-Raf^{+/+}$ (up) and $Kras^{+/+};Trp53^{F/F};hUBC-CreERT2^{+/T};c-Raf^{L/L}$ (down) mice at humane end point after continuous exposure to TMX. Scale bar, 0.05 mm.

(D) Body weight change in grams (g) of lung tumor-bearing male mice (circles) and female mice (triangles) exposed to TMX for 2 months. $Kras^{+/LSLG12V};Trp53^{F/F};hUBC-CreERT2^{+/T};c-Raf^{+/+}$ (solid circles (n=11) and solid triangles (n=9)) and $Kras^{+/FSFG12V};Trp53^{F/F};hUBC-CreERT2^{+/T};c-Raf^{L/L}$ (open circles (n=13) and open triangles (n=14)). Error bars indicate mean \pm SEM.

(E) Representative photos of tumor-bearing $Kras^{+/FSFG12V};Trp53^{F/F};hUBC-CreERT2^{+/T};c-Raf^{+/+}$ (Left) and $Kras^{+/LSLG12V};Trp53^{F/F};hUBC-CreERT2^{+/T};c-Raf^{L/L}$ (Right) mice after 2 months of TMX exposure.

Fur loss in $Kras^{+/LSLG12V};Trp53^{F/F};hUBC-CreERT2^{+/T};c-Raf^{L/L}$ mouse is caused by barbering behavior, a normal phenomenon observed in mice.

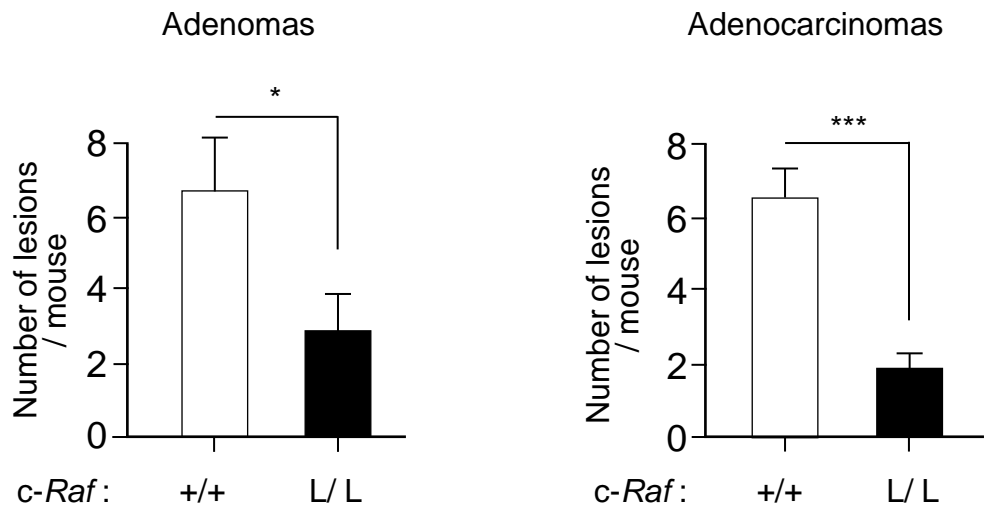
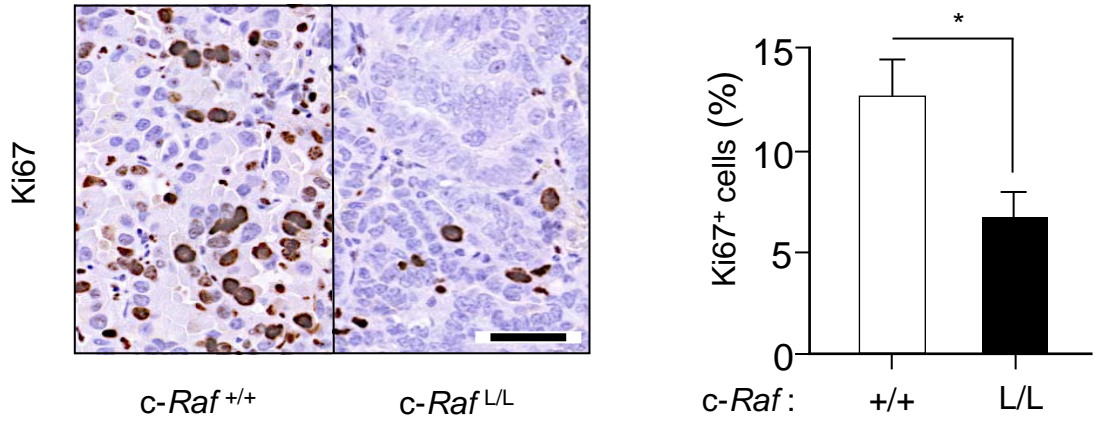
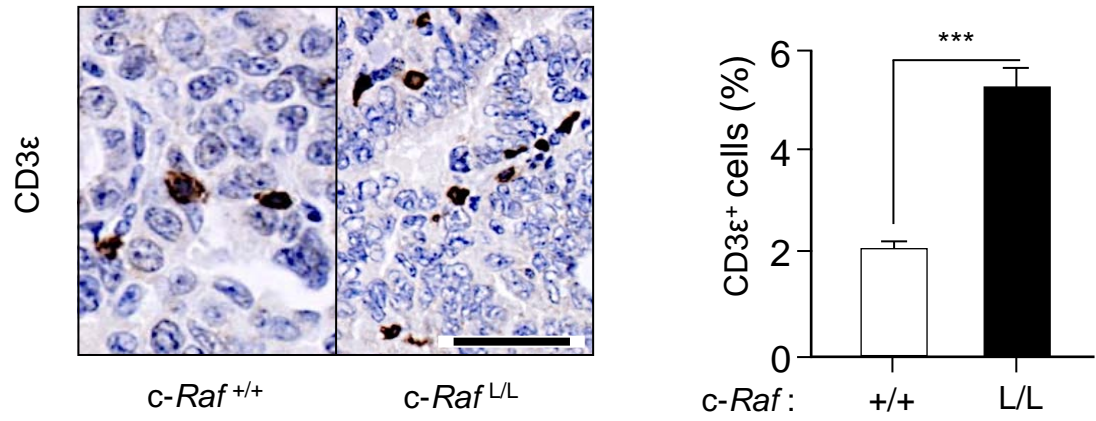
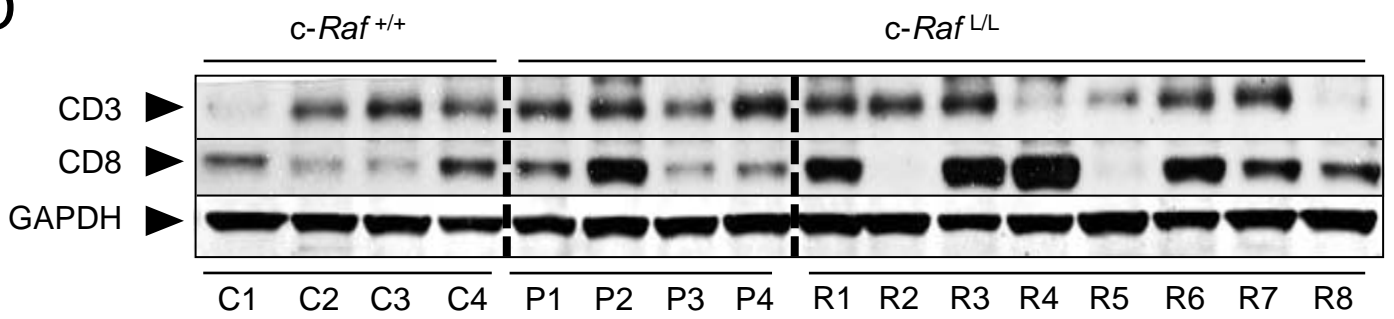
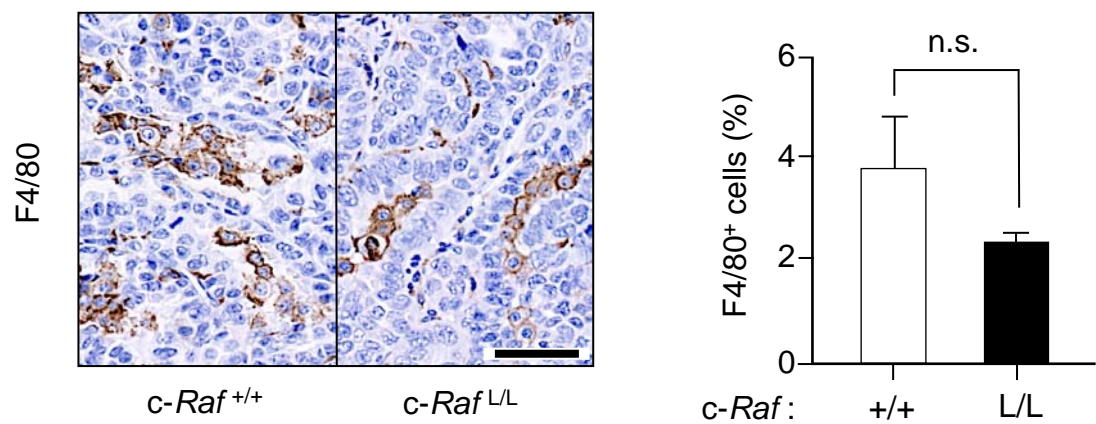
A**B****C****D****E**

Figure S4. c-RAF ablation prevents progression of established *Kras*^{G12V}/*Trp53* mutant lung tumors. Related to Figure 3.

(A) (Left) Quantification of number of adenomas and (Right) adenocarcinomas per mouse in *Kras*^{+FSFG12V};*Trp53*^{F/F};*hUBC-CreERT2*^{+T};*c-Raf*^{+/+} (open bar) and *Kras*^{+FSFG12V};*Trp53*^{F/F};*hUBC-CreERT2*^{+T};*c-Raf*^{L/L} tumor-bearing mice (n=6 per genotype) after 2 months of TMX exposure.

(B) (Left) Ki67 staining and (Right) quantification of Ki67⁺ cells in representative sections of paraffin embedded tumors of *Kras*^{+FSFG12V};*Trp53*^{F/F};*hUBC-CreERT2*^{+T};*c-Raf*^{+/+} (+/+ , open bar) and *Kras*^{+FSFG12V};*Trp53*^{F/F};*hUBC-CreERT2*^{+T};*c-Raf*^{L/L} (L/L, solid bar) mice (n=6 per genotype) treated with TMX for 2 months. Scale bar, 0.1 mm.

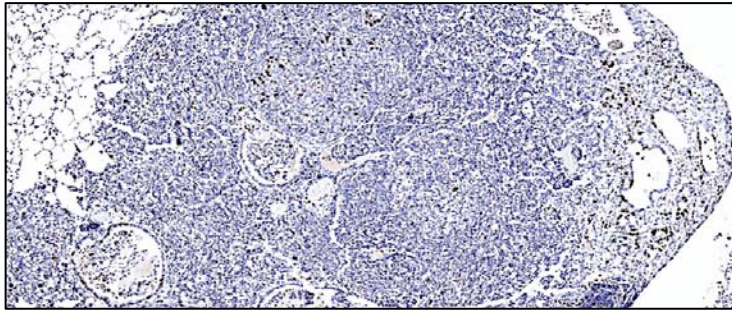
(C) (Left) CD3ε staining and (Right) quantification of CD3ε cells in representative sections of paraffin embedded tumors of *Kras*^{+FSFG12V};*Trp53*^{F/F};*hUBC-CreERT2*^{+T};*c-Raf*^{+/+} (+/+ , open bar) and *Kras*^{+FSFG12V};*Trp53*^{F/F};*hUBC-CreERT2*^{+T};*c-Raf*^{L/L} (L/L, solid bar) mice (n=6 per genotype) after 2 months of TMX exposure. Scale bar, 0.05 mm.

(D) Western blot analysis of CD3ε, and CD8, expression in lysates derived from individual tumors (C1 to C4) of control *Kras*^{+FSFG12V};*Trp53*^{F/F};*hUBC-CreERT2*^{+T};*c-Raf*^{+/+} mice and of *Kras*^{+FSFG12V};*Trp53*^{F/F};*hUBC-CreERT2*^{+T};*c-Raf*^{L/L} mice exposed to TMX for 2 months. Progressor (P1-P4) and regressor (R1-R8) tumors analyzed are indicated. GAPDH was used as loading control. Migration of the above proteins is indicated by arrowheads.

(E) (Left) F4/80 staining and (Right) quantification of F4/80⁺ cells in representative sections of paraffin embedded tumors of *Kras*^{+FSFG12V};*Trp53*^{F/F};*hUBC-CreERT2*^{+T};*c-Raf*^{+/+} (+/+ , open bar) and *Kras*^{+FSFG12V};*Trp53*^{F/F};*hUBC-CreERT2*^{+T};*c-Raf*^{L/L} (L/L, solid bar) mice (n=6 per genotype) after 2 months of TMX exposure. Scale bar, 0.05 mm.

Error bars indicate mean ± SEM. p values were calculated using the unpaired Student's T test. *p < 0.05 and ***p < 0.001. n.s.: not significant.

KI67 IHC



phospho-ERK IHC

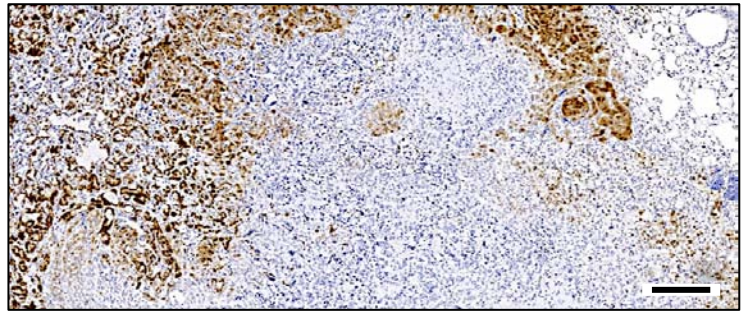
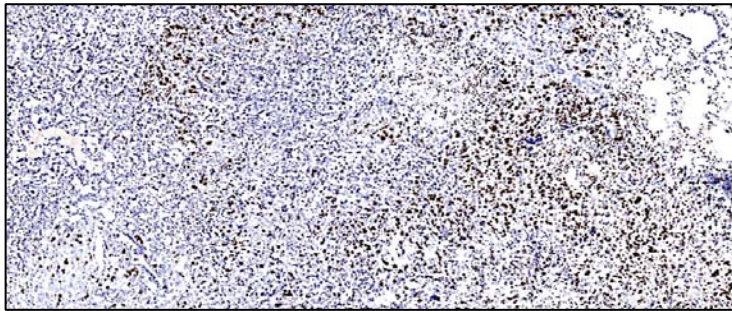
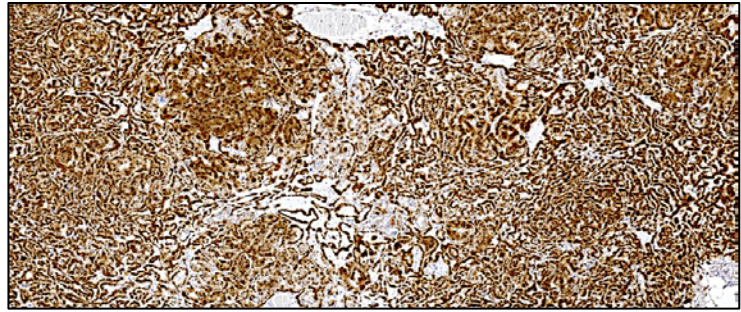
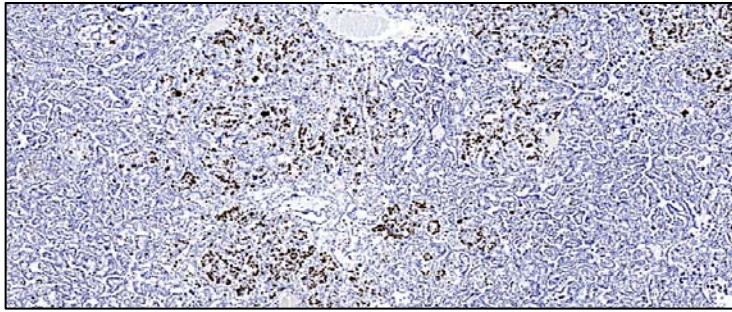
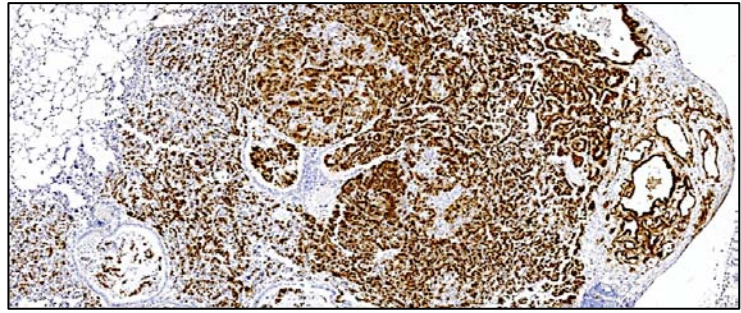


Figure S5. Phospho-ERK expression does not correlate with proliferation in *Kras*^{G12V}/*Trp53* mutant tumors after ablation of c-RAF. Related to Figure 4.

(Left) Ki67 staining and (Right) phospho-ERK staining in 3 representative sections of paraffin embedded *Kras*^{+/*FSFG12V*}; *Trp53*^{F/F}; *hUBC-CreERT2*^{+/*T*}; *c-Raf*^{L/L} tumors from 3 independent animals at 2 month of TMX exposure. Scale bar, 0.2 mm.

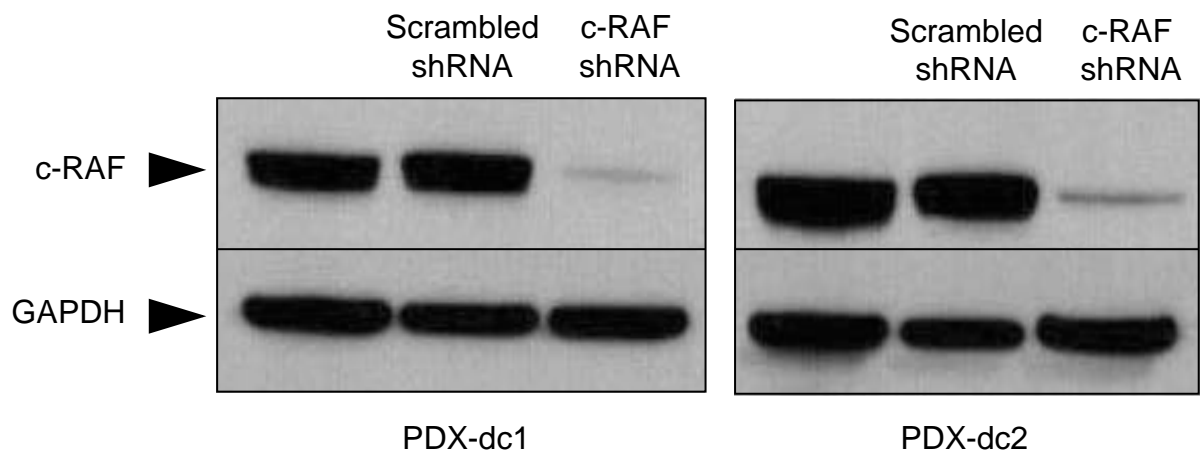


Figure S6. Effective c-RAF down-regulation in human tumor cells. Related to Figure 6.

Western blot analysis of c-RAF in 2 PDX-derived cell lines (PDX-dc1 and PDX-dc2) not infected and infected with lentiviral supernatants expressing a Scrambled shRNA, as control, and a shRNA against c-RAF at 2 weeks after the selection. GAPDH was used as loading control. Migration of the above mentioned proteins are indicated by arrowheads.